

# On the effect of wall slip on the determination of the yield stress of magnetorheological fluids

Jaime Caballero-Hernandez,<sup>1</sup> Ana Gomez-Ramirez,<sup>1</sup> Juan D.G. Duran,<sup>1</sup> F. Gonzalez-Caballero,<sup>1</sup> Andrey Yu. Zubarev,<sup>2</sup> and Modesto T. Lopez-Lopez<sup>1\*</sup>

<sup>1</sup>*Department of Applied Physics, Faculty of Sciences, University of Granada, 18071, Granada, Spain*

<sup>2</sup>*Department of Mathematical Physics, Ural Federal University, Lenina Ave 51, 620083, Ekaterinburg, Russia*

## Abstract

We study the effect of wall slip on the measured values of the yield stress of magnetorheological (MR) fluids. For this aim we used a rheometer provided with parallel-plate geometries of two types, distinguished by having smooth or rough surfaces. We found that wall slip led to the underestimation of the yield stress when measuring geometries with smooth surfaces were used, and that this underestimation was more pronounced for the static than for the dynamic yield stress. Furthermore, we analysed the effect that both irreversible particle aggregation due to colloidal interactions and reversible magnetic field-induced particle aggregation had on the underestimation provoked by wall slip. We found that the higher the degree of aggregation the stronger the underestimation of the yield stress. At low intensity of the applied magnetic field irreversible particle aggregation was dominant and, thus, the underestimation of the yield stress was almost negligible for well-dispersed MR fluids,

---

\* Author to whom correspondence should be addressed; electronic mail: modesto@ugr.es

whereas it was rather pronounced for MR fluids suffering from irreversible aggregation. As the magnetic field was increased the underestimation of the yield stress became significant even for the best dispersed MR fluid.

## **I. INTRODUCTION**

Magnetorheological (MR) fluids are suspensions of micron-size particles of magnetisable materials dispersed in a carrier fluid. Their main characteristic is the rapid and reversible change of their rheological behavior under the action of applied magnetic fields. This interesting property is known as MR effect and it is the base of many technological applications, such as MR clutches and dampers [1-6]. One of the main features of the MR effect is the tunability of the magnetic field-induced yield stress –the minimum shear stress required to induce flow. According to definition, we could distinguish two main types of yield stress: the static and dynamic yield stresses. For a structured suspension, the static yield stress is the minimum stress required to provoke the fracture of the suspension's structures in their weakest point; whereas, the dynamic yield stress is the stress required for the continuous breakage of the structures within the flow regime. Depending on the specific application, either dynamic or static yield stress is more important. On the other hand, controllable tunability of the yield stress within a large range is of crucial importance for most technological devices.

If not hindered, MR fluids suffer from strong irreversible particle aggregation, as a consequence of colloidal interactions between particles such as van der Waals attraction. Irreversible aggregation leads to the formation of large flocculi that settle out quickly, with the undesired result of the formation of sediments that are difficult to redisperse [7]. In applications, this results in the malfunctioning and lack of controllability of MR devices. Different approaches have been proposed to reduce

irreversible particle aggregation in MR fluids, such as the use of additives that impart steric repulsion to the dispersed particles, and the use of ionic liquids as carriers [8-12].

In a previous work we found that MR fluids also experience wall slip [13]. Wall slip phenomenon occurs because of the displacement of the dispersed particles away from the solid boundaries, leaving a lower-viscosity layer (slip layer) close to the measuring surfaces [14-15]. As a consequence, wall slip may alter the estimation of rheological parameters as the dynamic and static yield stress, giving rise to underestimation of these quantities. The use of measuring systems with rough surfaces has been, up to now, the best option to avoid wall slip effects in particulate suspensions [16-19]. In applications, wall slip may result in an imperfect transmittance of the yield stress to mobile parts of the MR devices, resulting in a lack of optimization of their functioning.

In spite of the importance of wall slip, a comprehensive study of the effect of wall slip on the yield stress of MR fluids is lacking in the literature. In this work we analyse the effect of wall slip on the measured (both dynamic and static) yield stresses of three MR fluids of different degree of irreversible particle aggregation. For this aim we compare the results obtained by using two parallel-plate measuring geometries with rough and smooth surfaces, respectively. The influence of the degree of irreversible particle aggregation as well as the magnetic field strength on the wall slip phenomenon are analysed in our work.

## **II. MATERIALS AND METHODS**

### **A. Materials**

We used iron particles (Fe-CC particles, BASF, Germany) as solid phase for the preparation of the MR fluids. According to the manufacturer, Fe-CC particles have a

silica coating and are spherical in shape with a median diameter of 5  $\mu\text{m}$ . We used two different carrier liquids, 1-ethyl-3-methylimidazolium diethylphosphate (Merck, Germany), which is an ionic liquid (IL), and mineral oil (MO) (Sigma Aldrich, Germany). The main properties of these liquids are included in Table 1. As surfactant for the preparation of one of the MR fluids, we used aluminum stearate (AlSt), supplied by Sigma Aldrich, Germany.

**Table 1:** *Physical properties of the ionic liquid (IL) and mineral oil (MO) used as carrier liquids.*

Carrier liquid	Viscosity at 25 $^{\circ}\text{C}$ (mPa·s)	Solubility in water	Density at 25 $^{\circ}\text{C}$ (g/cm <sup>3</sup> )	Conductivity (mS/cm)
IL	$317 \pm 16$	Yes	$1.14 \pm 0.01$	$0.66 \pm 0.03$
MO	$39.58 \pm 0.16$	No	$0.85 \pm 0.01$	---

Following the protocol described in Ref. [20], we prepared MR fluids according to three different compositions, all of them containing 50 vol.% of Fe-CC particles. MR fluid 1: Fe-CC particles in pure MO. MR fluid 2: Fe-CC particles in a 105 mM solution of AlSt in MO. MR fluid 3: Fe-CC particles in IL. Note that according to previous works [10-11], there are marked differences in the stability against irreversible particle aggregation of these compositions, with MR fluid 1 being the most aggregate composition and MR fluid 3 the least aggregate composition.

## B. Rheological measurements

We used a MCR300 controlled stress rheometer (Physica-Anton Paar, Germany) for the rheological measurements, provided with two different measuring system geometries, both of them parallel plate sets with 20 mm in diameter and a gap thickness of 0.35 mm. Measuring systems were differenced by the roughness of the surfaces of the plates, one of them having smooth surfaces and the other rough surfaces –for details on the roughness see [13]. For both measuring systems, we calibrated the rheometer by using two viscosity oil standards (Brookfield, USA) of 1.930 Pa s and 6.470 Pa s, to ensure that the measurements obtained could be safely compared.

We carried out steady-state measurements at  $10.0 \pm 0.1$  °C to obtain the static and dynamic yield stresses of the MR fluids in the presence of applied magnetic fields ranging in strength from 0 to 32 kA/m. For the application of the magnetic field we used a solenoid placed co-axially with the measuring geometry, as described in Ref. [21]. We performed three different types of measurements, which differed in the variable that was imposed, as described in what follows.

### ***1. Shear stress vs. imposed shear rate***

In this kind of experiments we imposed the shear rate,  $\dot{\gamma}$ , and monitored the corresponding shear stress,  $\sigma$ . To be precise, we proceeded according to the following steps. (i) preshear of the sample by a linear shear rate ramp in the range  $\dot{\gamma} = 0 - 100$  s<sup>-1</sup>, of 1 min of length, in the absence of magnetic field; (ii) waiting time of 30 s in the presence of an applied magnetic field; (iii) in the presence of the same applied field, shear rate ramp of 25 steps, in the range  $\dot{\gamma} = 0 - 300$  s<sup>-1</sup>, of a total length of 250 s – each imposed shear rate was maintained during 10 s. The corresponding shear stress was monitored and the values presented in this work are the mean ones for each imposed shear rate. From these experiments, we obtained curves of the shear stress as a

function of shear rate as this illustrated in Figure 1a. From this kind of curves we estimated the so-called dynamic yield stress,  $\sigma_y$ , by fitting the experimental data corresponding to the flow regime ( $\dot{\gamma} > 1 \text{ s}^{-1}$ ) to Bingham equation [22]:

$$\sigma = \sigma_y + \eta \dot{\gamma}. \quad (1)$$

In this equation both  $\sigma_y$  and  $\eta$  (known as dynamic viscosity) are fitting parameters.

## ***2. Imposed shear stress vs. shear rate***

In this kind of measurements we imposed the shear stress and monitored the corresponding shear rate. We used the following protocol. Preshear and waiting time as described in steps (i) and (ii) of the previous paragraph. Then, in the presence of applied magnetic field, a logarithmic stress ramp of 25 steps, of a total length of 250 s –each imposed shear stress was maintained during 10 s. The range of the stress ramp was adjusted in each experiment to cover the yield point and the surrounding areas. The corresponding shear rate was monitored and the values presented in this work are the mean ones for each imposed shear stress. This method (hereafter “method 1”) is the usual procedure to obtain the static yield stress. For this aim, the curve of shear stress as a function of shear rate is constructed, with the shear rate in logarithmic scale (see Figure 1b as an example). In this kind of curves, two closest points, with one belonging to the pre-yield regime ( $\dot{\gamma} \ll 1$ ) and the other to the post-yield (flow) regime ( $\dot{\gamma} > 1$ ) are identified (see Figure 1b). The first of these points (lower shear rate) corresponds to the maximum stress tolerated by the sample before breakage of the field-induced particle structures. The second point (higher shear rate) is the minimum stress required to induce the flow of the suspension, and is usually taken as the static yield stress. Note that the higher the number of points in the shear stress ramp, the more precise is the determination of the static yield stress by this procedure.

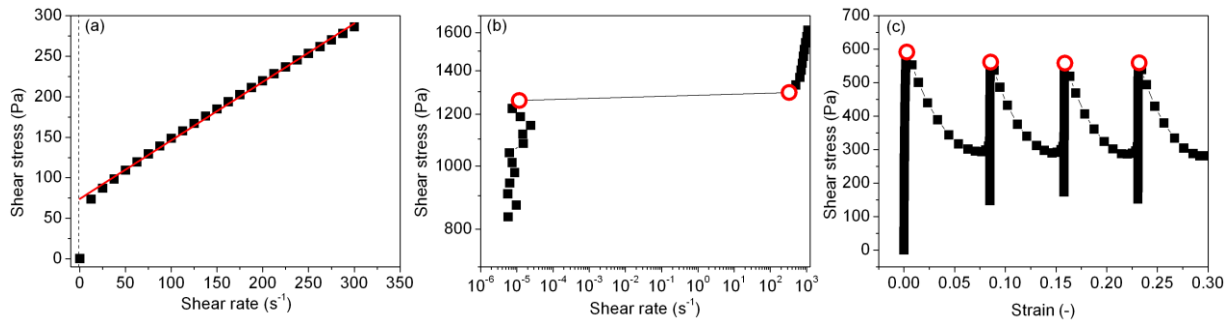


**Figure 1.** Different methods for the estimation of the yield stress. In all cases we used measuring geometry with rough surfaces. (a) Curve of shear stress vs. shear rate obtained by imposing the shear rate. Squares represent the experimental data and the solid line the best fit to Bingham equation. Experimental parameters: MR fluid 2; field strength  $H = 4$  kA/m. (b) Curve of shear stress vs. shear rate obtained by imposing the shear stress. Note the logarithmic scale in the  $x$ -axis. Symbols represent the experimental data. Note the two open circles, corresponding to the highest shear stress tolerated by the sample before fracture and the minimum shear stress required for inducing the flow of the suspension (yield stress). Experimental parameters: MR fluid 1; field strength  $H = 32$  kA/m. (c) Curve of shear stress vs. shear strain obtained by imposing the shear strain. Symbols represent the experimental data. Note the open circles, corresponding to the highest values of shear stress tolerated by the sample before fracture (yield stress). Experimental parameters: MR fluid 1; field strength  $H = 4$  kA/m.

### 3. Shear stress vs. imposed strain

In this kind of measurements we imposed the shear strain and monitored the corresponding shear stress. We used the following protocol. Preshear and waiting time as described in steps (i) and (ii) of the previous paragraph 1. Then, in the presence of

applied magnetic field, we imposed a ramp of shear strain,  $\gamma$ , within the range 0 – 0.30, of a total length of 10 s –each value of the shear strain was maintained during 0.01 s– and we monitored the corresponding shear stress. Curves of the shear stress as a function of shear strain consisted of a sequence of concave sections, as depicted in Figure 1c. The shape of each concave section of such a kind of curves, resembles the theoretical dependence of the shear stress as a function of shear strain usually obtained for the theoretical calculation of the yield stress of MR fluids –see for example Ref. [23]. The increasing branch of shear stress within each section corresponds to deformation and tilting with respect to the direction of the applied magnetic field of the field-induced particle structures. The maximum (peak) value corresponds to the highest value of the mechanical stress tolerated by the structures before breakage. Immediately after breakage, the shear stress decreases dramatically (in agreement with Figure 1c) until the particle structures rebuild by aggregation of broken structures as a consequence of magnetic attraction. The whole process of deformation, breakage and reconstruction starts again at this point. Then, the maximum stress within each section of the shear stress vs. shear strain curve corresponds to the static yield stress. In this work, we present the mean value of the successive peaks as static yield stress. We will refer to this method of measurement of the static yield stress as “method 2”.

### **III. RESULTS AND DISCUSSION**

In this section we will first make a comparison between the values of yield stress obtained by the three different methods: dynamic yield stress, static yield stress obtained by method 1, and static yield stress obtained by method 2. Then, we will analyse the effect that the wall slip has on the measured values of the dynamic yield



stress, depending on the aggregation state of the MR fluid. Finally, we will perform a similar analysis on the effect on the static yield stress.

#### **A. Comparison of the yield stress obtained by different methods**

As depicted in Figure 2 for MR fluid 1, both static and dynamic yield stresses increased as the magnitude of the applied magnetic field was increased, as expected for MR fluids. Similar results were obtained for the MR fluids 2 and 3, not shown here for brevity. For a detailed discussion on the effect of the magnetic field on the yield stress of concentrated MR fluids see Ref. [20]. Our experiments also indicated that when using smooth surfaces the yield stress obtained by the three different methods described in the experimental section approximately overlapped (Figure 2a). On the contrary, when we used rough surfaces there was a significant difference between the values of the dynamic yield stress and the static yield stress (Figure 2b). As observed, in this case (rough surfaces) the values of dynamic yield stress were considerably smaller than the values of the static yield stress. We can also conclude from data of Figure 2 that both methods of determination of the static yield stress (method 1 and method 2) gave approximately the same values.

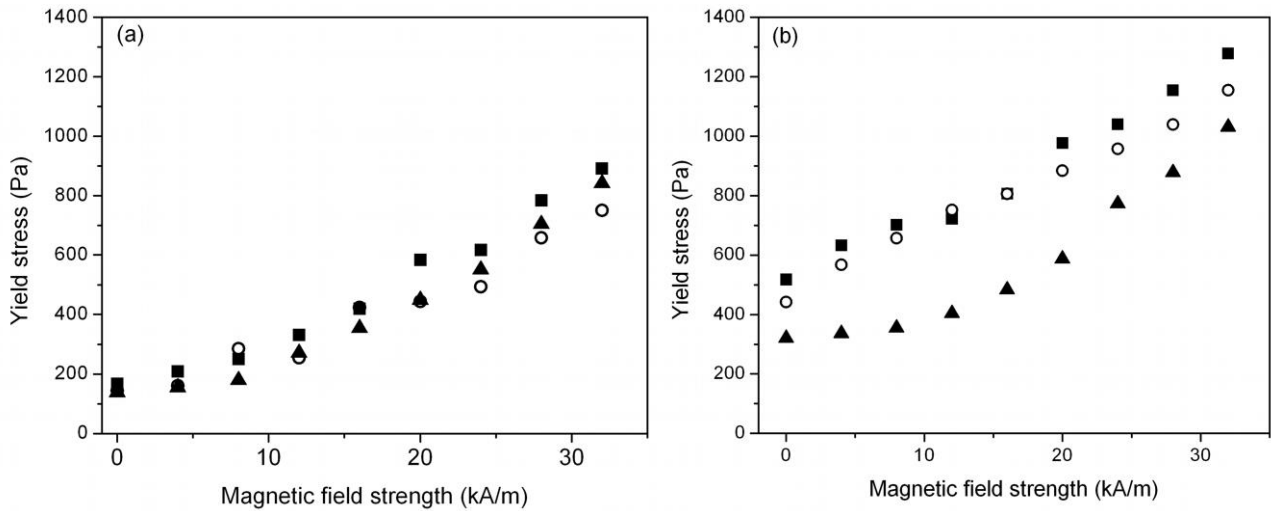


**Figure 2.** Yield stress of MR fluid 1 as a function of the applied magnetic field. ■: static yield stress obtained by method 1; ○: static yield stress obtained by method 2; ▲: dynamic yield stress. a) Yield stress obtained by means of geometry with smooth surfaces; b) yield stress obtained by means of geometry with rough surfaces.

### B. Effect of aggregation state on the measured values of the dynamic yield stress

In this subsection we analyse the effect that the state of aggregation of the MR fluid had on the measured values of the dynamic yield stress. For this we must take into account the irreversible aggregation between particles –resulting from colloidal interactions, such as van der Waals attraction. As mentioned in the experimental section, there were substantial differences in the state of irreversible aggregation between the three MR fluids used in our work, with MR fluid 1 being the most aggregated and MR fluid 3 being the best dispersed. In addition, we must keep in mind that apart from the irreversible particle aggregation resulting from colloidal interactions, there was also reversible field-induced aggregation under the application of a magnetic field.

In the case of MR fluid 1 there were significant differences for the whole range of applied magnetic field between the values of the dynamic yield stress obtained by geometries with rough surfaces and smooth surfaces, the former being considerably higher (Figure 3a). On the contrary, in the case of MR fluid 3 differences were almost negligible at low field and increased with the strength of the applied field, with the yield stress obtained by geometries with rough surfaces becoming progressively higher than the yield stress obtained by geometries with smooth surfaces.

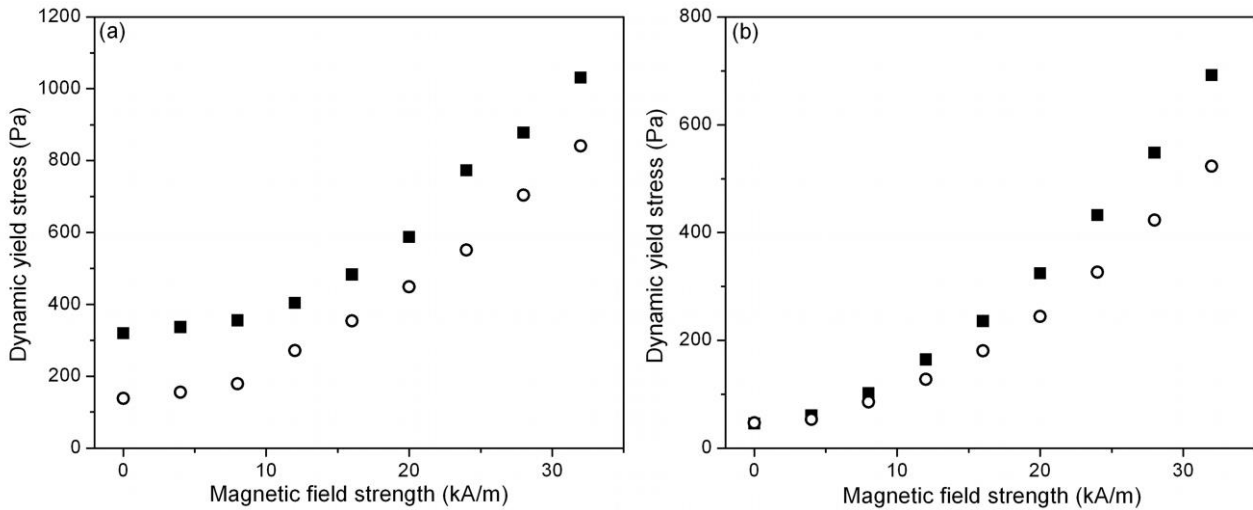


**Figure 3.** Dynamic yield stress as a function of the applied magnetic field. ■: Measurements by means of geometry with rough surfaces; ○: measurements by means of geometry with smooth surfaces. a) MR fluid 1; b) MR fluid 3.

From these results we can conclude that the underestimation of the values of the dynamic yield stress when using smooth surfaces was almost negligible in well-dispersed MR fluids at very low applied field. On the other hand, strong underestimation was obtained in the case of flocculated MR fluids, either by the action of colloidal interaction or the application of a magnetic field of high enough intensity.

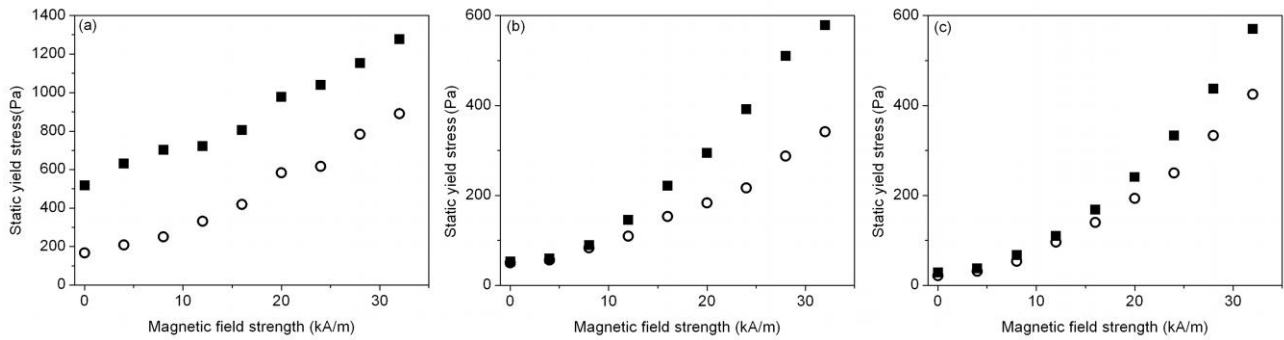


**Figure 4.** Static yield stress obtained by method 1 as a function of the applied magnetic field. ■: Measurements by means of geometry with rough surfaces; ○: measurements by means of geometry with smooth surfaces. a) MR fluid 1; b) MR fluid 2; c) MR fluid 3.

### C. Effect of aggregation state on the measured values of the static yield stress

Let us now analyse the effect that the state of aggregation between particles had in the measured values of the static yield stress. Figure 4 shows the results obtained by method 1 –note that similar results were obtained by method 2, not shown here for brevity. As observed, for the suspension with the higher degree of irreversible particle aggregation (MR fluid 1), there were large differences in the values of the static yield stress obtained by using geometries with smooth or rough surfaces. To be precise the values obtained by geometries with rough surfaces were higher by approximately 300-400 Pa, which implied an underestimation of the yield stress when using geometries with smooth surfaces of up to a factor of 3 at the lowest values of the applied field. On the other hand, differences in the values of the yield stresses determined by smooth and rough geometries were negligible at the lowest field strengths for the suspensions with better dispersion state (MR fluids 2 and 3). For these suspensions, however, as the

magnetic field strength was increased, the underestimation of the values of the static yield stress when using geometries with smooth surfaces increased (Figures 4b and 4c). As observed, this underestimation when using smooth surfaces was lighter the better the dispersion state, as observed by comparison of data for MR fluid 2 (worse dispersion) and MR fluid 3 (better dispersion).

#### **IV. CONCLUSIONS**

We have shown that wall slip leads to the underestimation of the magnetic field-induced yield stress of MR fluids when measuring geometries with smooth surfaces are used. This underestimation is most important for the static yield stress than for the dynamic yield stress, which is in agreement with the established knowledge that wall slip in particulate suspensions happens mainly at low shear rate values, before the flow of the suspensions [14]. Furthermore, we have shown that the underestimation of the yield stress due to the wall slip is more important the higher the aggregation degree of the suspensions. In this sense, both irreversible particle aggregation due to colloidal interactions (such as van der Waals attraction) and magnetic field-induced particle aggregation lead to underestimation of the yield stress, although the effect of the former type of aggregation seems to be dominant at low enough magnetic field strength. These conclusions should be carefully considered in practical applications of MR fluids that benefit from a high yield stress, such as MR clutches and dampers. When designing such a kind of devices, the used of rough surfaces should be considered for chambers containing MR fluids, in order to diminish the effect of wall slip and, consequently, to maximize the transmittance of the yield stress to mobile parts of the devices. Special care should be taken with surfaces moving at low speed and in the case of concentrated MR fluids that will likely suffer from irreversible particle aggregation.

## **ACKNOWLEDGMENTS**

This study was supported by project FIS2013-41821-R (Plan Nacional de Investigación Científica, Desarrollo e Innovación Tecnológica, Ministerio de Economía y Competitividad, Spain, co-funded by ERDF, European Union), by the Russian Science Foundation, project 14-19-00989 and by Program of Ministry of Science and Education of the Russian Federation, project 3.12.2014/K

## **References**

- [1] Ginder JM: Rheology controlled by magnetic fields *Enc. Appl. Phys.* 16 (1996) , 487–503.
- [2] Lopez-Lopez MT, Rodriguez-Arco L, Duran JDG, Gonzalez-Caballero F: 14th International Conference on Electrorheological Fluids and Magnetorheological Suspensions (ERMR2014) *Appl. Rheol.* 24 (2014) 55-57.
- [3] Lopez-Lopez MT, Gonzalez-Caballero F: Preface: 14th International Conference on Electrorheological Fluids and Magnetorheological Suspensions. *J. Intell. Mater. Syst. Struct.* 26 (2015) 1755-1756.
- [4] Park BJ, Fang FF, Choi HJ: Magnetorheology: materials and application. *Soft Matter* 6 (2010) 5246–5253.
- [5] Phulé PP, Ginder JM: The materials science of field-responsive fluids. *MRS Bull.* 23 (1998) 19–21.
- [6] Wereley N. (Editor): *Magnetorheology: Advances and Applications* (The Royal Society of Chemistry, Cambridge, 2014).

- [7] Phulé PP, Mihalcin MT, Gene S: The role of the dispersed-phase remnant magnetization on the redispersibility of magnetorheological fluids. *J. Mater. Res.* 14 (1999) 3037-3041.
- [8] Altin E, Gradl J, Peukert W: First studies on the rheological behavior of suspensions in ionic liquids. *Chem. Eng. Technol.* 29 (2006) 1347-1354.
- [9] Charles SW: The Preparation of Magnetic Fluids. *Lect. Notes Phys.* 594 (2002) 201–230.
- [10] Gómez-Ramírez A, López-López MT, González-Caballero F, Durán JDG: Stability of magnetorheological fluids in ionic liquids. *Smart Mater Struct* 20 (2011) 045001–045010.
- [11] López-López MT, Zugaldía A, González-Caballero F, Durán JDG: Sedimentation and redispersión phenomena in iron-based magnetorheological fluids. *J. Rheol.* 50 (2006) 543–560.
- [12] Guerrero-Sanchez C, Lara-Ceniceros T, Jiménez-Regalado E, Rasa M, Schubert US: Magnetorheological Fluids Based on Ionic Liquids. *Adv. Mater.* 19 (2007) 1740–1747.
- [13] Gómez-Ramírez A, López-López MT, González-Caballero F, Durán JDG: Wall slip phenomena in concentrated ionic liquid-based magnetorheological fluids. *Rheol Acta* 51 (2012) 793-803.
- [14] Barnes HA: A review of the slip (wall depletion) of polymer solutions, emulsions and particle suspensions in viscometers: its cause, character, and cure. *J. Non-Newtonian Fluid Mech.* 56 (1995) 221-251.
- [15] Buscall R: Letter to the Editor: Wall slip in dispersion rheometry. *J. Rheol.* 54 (2010) 1177-1183.

- [16] Buscall R, McGowan JJ, Morton-Jones AJ: The rheology of concentrated dispersions of weakly-attracting colloidal particles with and without wall slip. *J. Rheol.* 37 (1993) 621–641.
- [17] Carotenuto C, Vananroye A, Vermant J, Minale M. Predicting the apparent wall slip when using roughened geometries: A porous medium approach. *J. Rheol.* 59 (2015) 1131-1150.
- [18] Gregory T, Mayers S: A note on slippage during the study of the rheological behaviour of paste inks. *Surf Coat Int JOCCA* 76 (1993) 82–86.
- [19] Isa L, Besseling R, Poon WCK: Shear zones and wall slip in the capillary flow of concentrated colloidal suspensions. *Phys. Rev. Lett.* 98 (2007) 198305.
- [20] López-López MT, Kuzhir P, Caballero-Hernández J, Rodríguez-Arco L, Durán JDG, Bossis G: Yield stress in magnetorheological suspensions near the limit of maximum-packing fraction. *J. Rheol.* 56 (2012) 1209-1224.
- [21] Kuzhir P, López-López MT, Vertelov G, Pradille C, Bossis G: Shear and squeeze rheometry of suspensions of magnetic polymerized chains. *Rheol. Acta* 47 (2008) 179-187.
- [22] Barne HA: Shear-Thickening (“Dilatancy”) in Suspensions of Non-aggregating Solid Particles Dispersed in Newtonian Liquids. *J. Rheol.* 33 (1989) 329-366.
- [23] Bossis G, Lemaire E, Volkova O, Clercx HJH: Yield stress in magnetorheological and electrorheological fluids: A comparison between microscopic and macroscopic structural models. *J. Rheol.* 41 (1997) 687-704.



## Figure Captions

**Figure 1.** Different methods for the estimation of the yield stress. In all cases we used measuring geometry with rough surfaces. (a) Curve of shear stress vs. shear rate obtained by imposing the shear rate. Squares represent the experimental data and the solid line the best fit to Bingham equation. Experimental parameters: MR fluid 2; field strength  $H = 4$  kA/m. (b) Curve of shear stress vs. shear rate obtained by imposing the shear stress. Note the logarithmic scale in the  $x$ -axis. Symbols represent the experimental data. Note the two open circles, corresponding to the highest shear stress tolerated by the sample before fracture and the minimum shear stress required for inducing the flow of the suspension (yield stress). Experimental parameters: MR fluid 1; field strength  $H = 32$  kA/m. (c) Curve of shear stress vs. shear strain obtained by imposing the shear strain. Symbols represent the experimental data. Note the open circles, corresponding to the highest values of shear stress tolerated by the sample before fracture (yield stress). Experimental parameters: MR fluid 1; field strength  $H = 4$  kA/m.

**Figure 2.** Yield stress of MR fluid 1 as a function of the applied magnetic field. ■: static yield stress obtained by method 1; ○: static yield stress obtained by method 2; ▲: dynamic yield stress. a) Yield stress obtained by means of geometry with smooth surfaces; b) yield stress obtained by means of geometry with rough surfaces.

**Figure 3.** Dynamic yield stress as a function of the applied magnetic field. ■: Measurements by means of geometry with rough surfaces; ○: measurements by means of geometry with smooth surfaces. a) MR fluid 1; b) MR fluid 3.

**Figure 4.** Static yield stress obtained by method 1 as a function of the applied magnetic field. ■: Measurements by means of geometry with rough surfaces; ○: measurements by means of geometry with smooth surfaces. a) MR fluid 1; b) MR fluid 2; c) MR fluid 3.